Published in final edited form as:
Gene Expr Patterns. 2007 April ; 7(5): 606–613.

Pax6 is misexpressed in *Sox1* null lens fiber cells

Amy L. Donner*, **Fang Ko**[a], **Vasso Episkopou**[b], and **Richard L. Maas**
Division of Genetics, Department of Medicine, Brigham and Women's Hospital and Harvard Medical School, NRB 458, 77 Louis Pasteur Avenue, Boston, MA 02115, USA

Abstract

Sox1 null lens fiber cells fail to elongate and have disrupted expression of *gamma crystallin*. We have evaluated the expression of Sox1 and Pax6 proteins during critical stages of lens morphogenesis, with particular focus on fiber cell differentiation. While Pax6 and Sox1 are co-expressed during early stages of fiber cell differentiation, Sox1 up-regulation coincides temporally with the down-regulation of Pax6, and these proteins therefore display a striking inverse expression pattern in the lens fiber cell compartment. Furthermore, Pax6 is inappropriately expressed in the fiber cells of *Sox1* null mice and the Pax6 target, α5 integrin, is simultaneously misexpressed. Finally, we demonstrate a genetic interaction between *Sox1* and *Pax6*, as *Sox1* heterozygosity partially rescues the diameter of $Pax6^{Sey}$ lenses by increasing the number of cells in the fiber cell compartment.

Keywords

Sox1; *Pax6*; α5 integrin; cataract; lens; fiber cell; anterior epithelial layer

1. Results and Discussion

The vertebrate lens is composed of two major cell types, epithelial cells and fiber cells. During development, the lens vesicle is polarized into anterior and posterior compartments. Cells in the posterior lens exit the cell cycle and elongate to form primary fiber cells, while cells in the anterior lens differentiate into epithelium. A subset of anterior epithelial layer (AEL) cells proliferate and their daughters subsequently exit the cell cycle, migrate into the transition zone and differentiate into secondary fiber cells.

Sox1, a Group B1 SRY-like HMG box transcription factor, is required for fiber cell development in mice (Nishiguchi et al., 1998). Mice lacking *Sox1* have small, opaque lenses with a persistent hole in the central cavity where fiber cells fail to fully differentiate (Nishiguchi et al., 1998). *Sox1* null lenses lose expression of *γ-crystallin* at E12.5 coincident with the down-regulation of the related gene, *Sox2* (Nishiguchi et al., 1998). Although loss of *γ-crystallin* has been linked to cataract formation (reviewed in Graw, 2004), it is reasonable to hypothesize that other genes downstream of *Sox1* also contribute to the fiber cell differentiation defect.

In addition to Sox1, other transcription factors are necessary for proper fiber cell differentiation, including *Pax6, c-Maf, Pitx3, Prox1*, and *FoxE3*. Mutation of these factors causes cataracts in

*Corresponding author: adonner@rics.bwh.harvard.edu, Phone: (617) 525-4710, FAX: (617) 525-4751.
[a]Current address: Johns Hopkins School of Public Health, Baltimore, MD, USA
[b]Mammalian Neurogenesis Group, MRC Clinical Sciences Centre, Imperial College School of Medicine, Hammersmith Hospital Campus, Du Cane Rd., London W12 0NN, UK

both mouse models and humans (Glaser et al., 1994; Hanson et al., 1994; Semina et al., 1998; Wigle et al., 1999; Blixt et al., 2000; Brownell et al., 2000; Duncan et al. 2000; Ring et al., 2000; Semina et al., 2000, 2001; Jamieson et al., 2002; Lyon et al., 2003; Berry et al., 2004; Duncan et al., 2004; Rajaram and Kerpolla, 2004). Most of these transcription factors are downstream of *Pax6* in the lens. (Brownell et al., 2000; Dimanlig et al., 2001; Sakai et al., 2001; Chauhan et al., 2002; Reza et al., 2002).

The central role that *Pax6* plays in lens development and its relationship with another GroupB1 SRY-like HMG box protein, Sox2, is well documented (Kamachi et al., 2001; Aota et al., 2003; Kondoh et al., 2004; Donner et al., in press). *Pax6* is upstream of *Sox2* (Furuta and Hogan, 1998), Pax6 and Sox2 cooperatively regulate gene expression (Kamachi et al. 2001, Aota et al., 2003), and *Sox2* is required for the maintenance of Pax6 (Donner et al., in press). Appropriate temporal, spatial, and quantitative control of *Pax6* expression is required for appropriate lens morphogenesis (Hill *et al.*, 1991; Glaser et al., 1994; Hanson et al., 1994; Grindley et al., 1995; Quinn et al., 1996; Schedl et al., 1996; Brown et al., 1998; Ashery-Padan et al., 2000; Duncan et al., 2000; van Raamsdonk and Tilgham, 2000; Dimanlig *et al.*, 2001; Duncan et al., 2004). *PAX6* mutation is causative for several congenital eye defects in humans including aniridia, Peters' anomaly and cataract (reviewed in Prosser and van Heyningen, 1998). Given the importance of the Pax6 for appropriate lens morphogenesis and the link between Pax6 and Sox2, we sought to evaluate the relationship between Sox1 and Pax6 in the developing lens.

1.1. Fiber cell expression of Sox1 and Pax6 is inversely correlated

We assessed the expression of Sox1 and Pax6 during fiber cell formation and differentiation. At E11.5, Sox1 was first detected in cells in the posterior lens, while Pax6 was expressed in all cells of the lens pit (Fig. 1A–C). By E12.5, primary fiber cells elongated across the lens vesicle and their nuclei were anteriorly translocated. While Sox1 and Pax6 are still expressed in most nuclei at this stage, Sox1 staining increased and the intensity of Pax6 staining diminished in the fiber cell compartment as compared to E11.5 (Fig. 1D–F). At E13.5, Sox1 persisted in fiber cell nuclei, while Pax6 was further down regulated with weakest expression observed in the center of the lens (Fig. 1G–I). By E15.5, Pax6 was no longer detected in fiber cell nuclei while Sox1 expression remained (Fig. 1J–L). From E12.5 to E15.5 Sox1 and Pax6 are co-expressed in the AEL (Fig. 1D, 1F–G, 1I–J, 1L). At the onset of primary fiber cell differentiation, Sox1 and Pax6 are co-expressed, but thereafter Pax6 is down regulated while Sox1 is up regulated and maintained. Thus, while Sox1 and Pax6 are co-expressed in the AEL, they exhibit a transiently overlapping, but subsequently inverse expression pattern in the lens fiber cell compartment.

1.2. Pax6 expression persists inappropriately in the fiber cells of Sox1$^{-/-}$ lenses

We next assessed Pax6 expression in *Sox1*$^{-/-}$ eyes. The disruption in fiber cell differentiation in *Sox1*$^{-/-}$ lenses is evident by E12.5. Unlike wild-type lenses, neither fiber cell elongation nor anterior translocation of nuclei has occurred (Fig. 2A–B). By E13.5, some fiber cell elongation and anterior movement of nuclei was evident in *Sox1*$^{-/-}$ lenses (Fig. 2C–D). Pax6 expression was inappropriately maintained in posterior cells of the *Sox1*$^{-/-}$ lens through at least E15.5 (Fig. 2A–F), even after the delayed onset of fiber cell elongation. Sox2 was undetectable in both wild-type and *Sox1*$^{-/-}$ mice at E12.5 (data not shown), and thus cannot be responsible for the persistence of Pax6. Thus, *Sox1* is required for the appropriate repression of Pax6 in differentiating lens fiber cells.

1.3. α5 integrin, a Pax6 target, is inappropriately maintained in Sox1 null fiber cells

The persistent and inappropriate expression of the transcription factor Pax6 in the fiber cell compartment of *Sox1*$^{-/-}$ lenses suggests that factors downstream of Pax6 might also be

maintained. The fiber cell differentiation markers α5 and β1 integrin are a co-receptor for fibronectin and are direct downstream targets of Pax6 in the lens (Johansson et al., 1997; Duncan et al., 2000). No major abnormalities were observed in β1 integrin expression in *Sox1*$^{-/-}$ lenses at E13.5 or 15.5 (data not shown). Thus, misexpression of β1 integrin does not contribute to the *Sox1*$^{-/-}$ lens phenotype.

The expression of α5 integrin was dynamic during fiber cell differentiation (Fig. 3A–D). At E13.5, α5 integrin was expressed throughout the AEL, the equatorial transition zone, and the fiber cell compartment (Fig. 3A), while α5 integrin expression was reduced in the fiber cell compartment at E15.5 (Fig. 3C). The temporal pattern of α5 integrin expression resembled that of Pax6, which diminished in the fiber cell compartment at E12.5 (Fig. 1D, Fig. 2A) and was absent from the fiber cell compartment by E15.5 (Fig. 1J, Fig. 2E). Down-regulation of α5 integrin began later than that of Pax6, but was complete by E15.5 (Fig. 3C).

Sox1$^{-/-}$ lenses differed from wild-type lenses in their pattern of α5 integrin expression. At E13.5, as in wild-type lenses, α5 integrin was found in the AEL, the equatorial transition zone, and the fiber cell compartment (Fig. 3B). Unlike wild-type lenses, however, α5 integrin was not down regulated in the fiber cell compartment at E15.5, but persisted (Fig. 3D). Moreover, the persistence of α5 integrin expression followed the pattern of Pax6 expression (compare Figs. 2D, 2F to Figs. 3B, 3D). Thus, in *Sox1*$^{-/-}$ fiber cells at E15.5, both Pax6 and α5 integrin expression persist inappropriately.

1.4. Loss of Sox1 partially rescues the size of Pax6$^{Sey/+}$ lenses

To test whether *Pax6* and *Sox1* interact at the genetic level during fiber cell differentiation, we assessed the histology of lenses with compound *Pax6* and *Sox1* mutations at E13.5 (Fig. 4A–F), the stage of lens development when Pax6 misexpression was first evident in the *Sox1*$^{-/-}$ fiber cells. Both the *Sox1*$^{-/-}$ phenotype and the *Pax6*$^{Sey/+}$ phenotype were evident at E13.5 (Fig. 4C–D). The lenses of *Pax6*$^{Sey/+}$ mice were misshapen and significantly smaller when compared to those in wild-type mice (maximum lens diameter on dorsal/ventral axis: 307 ± 9.7 microns (mean ± SD, n=5) and 459 ± 21 microns respectively, $p < .001$) (Fig. 4A, 4D–D', 4G). The *Sox1*$^{-/-}$ lenses were also smaller than wild-type lenses and had a large hole between the elongating fiber cells and the AEL resulting from a failure in primary fiber cell differentiation (Fig 4A, 4C). Both *Pax6*$^{Sey/+}$ and *Sox1*$^{+/-}$*; Pax6*$^{Sey/+}$ lenses had variable phenotypes including small lenses and a persistent stalk connecting the lens AEL to the corneal ectoderm (Fig. 4D–E, and data not shown). Lens defects in *Sox1*$^{+/-}$*; Pax6*$^{Sey/+}$ mice, however, were milder than the *Pax6*$^{Sey/+}$ phenotypes. The *Sox1*$^{+/-}$; *Pax6*$^{Sey/+}$ lenses were larger and less conical in shape than the *Pax6*$^{Sey/+}$ lenses (maximum lens diameters 368 ± 28 microns and 307 ± 9.7 microns, respectively, $p < .01$) (Figure 4D–4D', 4E–4E', 4G). Thus, reduction in *Sox1* dosage partially rescued the size of *Pax6*$^{Sey/+}$ lenses, with the increased lens size resulting from an increase in either fiber cell number or fiber cell elongation. These data demonstrate a genetic interaction between *Sox1* and *Pax6*, and are consistent with *Pax6* and *Sox1* having opposing affects on fiber cell differentiation.

Pax6$^{Sey/+}$*; Sox1*$^{-/-}$ compound mutant lenses were small and grossly misshapen like *Pax6*$^{Sey/+}$ lenses (Fig. 4F–F'). In addition, the AEL in the *Pax6*$^{Sey/+}$*; Sox1*$^{-/-}$ lenses was multi-layered and disorganized (Fig. 4F–F'). Thus, unlike the partial rescue observed in lenses with combined heterozygous mutations in *Pax6* and *Sox1*, the combination of *Pax6*$^{Sey/+}$ and *Sox1*$^{-/-}$ had an additive detrimental effect on both lens size and organization of the AEL.

1.5. Pax6$^{Sey/+}$; Sox$^{+/-}$ lenses have more fiber cells than those of Pax6$^{Sey/+}$ mice

To determine whether an increase in fiber cell number contributed to the increase in size of *Pax6*$^{Sey/+}$*; Sox1*$^{-/-}$ lenses as compared to *Pax6*$^{Sey/+}$ lenses, we counted nuclei in the fiber cell

compartments of wild-type, *Sox1*$^{+/-}$, *Pax6*$^{Sey/+}$ and *Sox1*$^{+/-}$; *Pax6*$^{Sey/+}$ lenses. To facilitate in the discrimination between fiber cells and epithelial cells, we stained the sections with the epithelial-specific marker, E-cadherin, and the nuclear marker, DAPI. We counted the nuclei of cells that were negative for E-cadherin expression. The fiber cell nuclei number in *Sox1*$^{+/-}$; *Pax6*$^{Sey/+}$ lenses was statistically significantly higher than in *Pax6*$^{Sey/+}$ lenses (fiber cell number 190 ± 31 and 144 ± 13 (mean ± SD), respectively, $p < 0.001$) (Fig 5E). Thus, the increase in size observed in *Sox1*$^{+/-}$; *Pax6*$^{Sey/+}$ lenses versus *Pax6*$^{Sey/+}$ lenses is due, at least in part, to an increase in fiber cell number.

1.6. Sox1 and Pax6 have both additive and antagonistic activities in the lens

Interestingly *Sox1*$^{-/-}$; *Pax6*$^{Sey/+}$ lenses are more severely affected than either *Sox1*$^{-/-}$ or *Pax6*$^{Sey/+}$ lenses alone. Thus, combined *Sox1* and *Pax6* loss-of-function both rescue and disrupt lens development. This result could be reconciled by additive defects in the cells of the AEL in *Sox1*$^{-/-}$; *Pax6*$^{Sey/+}$ lenses, which normally maintain both *Pax6* and *Sox1*. The AEL of the *Sox1*$^{-/-}$; *Pax6*$^{Sey/+}$ lens is multi-layered (Fig. 4F–F'). Abnormal morphology of the AEL was also observed in *Pax6*$^{Sey/+}$ lenses (Fig. 4D–D', pointed appearance) although the phenotype was most pronounced in the *Sox1*$^{-/-}$; *Pax6*$^{Sey/+}$ AEL. This is consistent with the findings of Collinson et al. (2001) that *Pax6*$^{Sey/+}$ cells are preferentially lost from the AEL between E12.5 and E16.5 in *Pax6*$^{Sey/+}$ ↔ *Pax6*$^{+/+}$ chimeric mice. Additional evidence that this additive defect derives from a defect in the AEL comes from lenses evaluated at E15.5. By this stage, secondary fiber cells derived from the AEL are present. At this stage, wild-type, *Pax6*$^{Sey/+}$, *Sox1*$^{+/-}$; *Pax6*$^{Sey/+}$ lenses have phenotypes comparable to those described at E13.5, although the lenses are larger (Fig. 6A–C). In contrast, the *Sox1*$^{-/-}$; *Pax6*$^{Sey/+}$ lenses are more severely affected at E15.5 (Fig. 6D). The lenses are small and there is no clear delineation between the AEL and the fiber cell compartment. The increase in severity in phenotype between E13.5 and E15.5 indicates that the *Sox1*$^{-/-}$; *Pax6*$^{Sey/+}$ lens has a progressively degenerative phenotype. Thus, both *Sox1* and *Pax6* play an important role in organization or maintenance of the AEL and combined loss-of-function of these genes has an additive detrimental effect on the AEL.

2. Experimental Procedures

2.1. Mouse work

All mouse work was performed in accordance with protocols approved by the Harvard Animal Care and Usage Committee. *Sox1*$^{\beta geo}$, *Sox1*^{M1}, and *Pax6*$^{1\text{-}NeuSey/+}$ (*Pax6*$^{Sey/+}$) mice were maintained on a C3H/HeN background (Nishiguchi et al., 1998; Ekonomou et al., 2005). *Sox1*$^{\beta geo}$ and *Sox1*^{M1} heterozygotes (*Sox1*$^{+/-}$) were crossed to generate *Sox1*$^{-/-}$ embryos (Ekonomou et al., 2005). *Sox1*$^{+/-}$ mice were crossed to *Pax6*$^{Sey/+}$ mice. Double heterozygotes resulting from these crosses were bred to *Sox1*$^{+/-}$ mice. Appropriately staged embryos and their extra-embryonic tissues were collected, and genomic DNA from extra-embryonic tissue was screened by PCR (Nishiguchi et al., 1998). The *Pax6*$^{1\text{-}NeuSey/+}$ allele was identified by a PCR fragment polymorphism producing a *Hinc*II restriction site.

2.2. Immunofluorescence

Embryos were embedded in paraffin or frozen in OCT (Tissue-Tek). In Fig. 1, stage E11.5 and E13.5 embryos were prepared from frozen sections, while paraffin embedded embryos were utilized to improve histology on eyes at E12.5 and E15.5. In Fig. 2, stage E12.5 and E15.5 sections were prepared from paraffin sections, while frozen embryos were utilized for E13.5. For Fig. 3 and Fig. 5 frozen sections were utilized.

For frozen sections, embryos were fixed in 4% paraformaldehyde (PFA) for 1 hour, equilibrated in 30% sucrose and embedded in OCT. For paraffin sections, embryos were fixed in 4% PFA overnight, dehydrated, and embedded in wax. Sox1 immunofluorescence in paraffin

sections required trypsin unmasking (Sigma). Pax6 staining in paraffin (DSHB 1:50, mouse concentrate) was performed as described (Collinson et al., 2003). All frozen sections were unmasked by boiling in Antigen Unmasking Solution (Vector Laboratories) unless otherwise indicated. Sox1 expression in the epithelium was not detectable. The quality of unmasking varied slightly and accounts for the loss of low-level Pax6 staining in some sections. Comparable panels in each figure were always treated together to standardize the quality of unmasking. Staining for β1 integrin (Santa Cruz), α5 integrin (Santa Cruz) and E-cadherin (Zymed® Laboratories) were performed on frozen sections. Detection of α5 and β1 integrin required unmasking in 1mg/mL pepsin; 2.8% glacial acetic acid, pH 3.0 at room temperature.

Indirect visualization was achieved using secondary antibodies with fluorescent conjugates [anti-rabbit Cy3, anti-goat Cy3 (Jackson Immunologicals) and anti-rabbit Alexa-Fluor 488 (Molecular Probes)]. Sections were mounted with Vectashield® plus DAPI (Vector Laboratories), visualized on a Zeiss Axiophot microscope, and photographed with a Leica DFC350 F Digital Camera.

2.3. Histology, maximum diameter calculations, and fiber cell quantification

For maximum diameter calculations, serial transverse paraffin sections from wild-type, compound heterozygous *Sox1*$^{+/-}$; *Pax6*$^{Sey/+}$ and *Pax6*$^{Sey/+}$ mutants were cut through 5 embryos of each genotype. Sections were H&E stained by standard protocols (Nagy et al., 2003). The diameter of each lens was measured from the AEL to the posterior of the fiber cell compartment and the maximum diameters were averaged. A single factor ANOVA and post-hoc Sheffe's test were utilized to determine the statistical significance of lens maximum diameter differences (wild-type$_1$ 459 ± 21 microns, *Pax6*$^{Sey/+}{}_2$ 307 ± 9.7 microns, and *Sox1*$^{+/-}$, *Pax6*$^{Sey/+}{}_3$ 368 ± 28 microns; mean ± SD). Maximum lens diameters for wild-type, *Pax6*$^{Sey/+}$ and *Pax6*$^{Sey/+}$; *Sox1*$^{+/-}$ lenses are statistically different. (n=5 per genotype, $p < 0.05$, $F_{.05}$ (2, 12)=3.88; F_{12}=64.4, F_{13}=23.1, F_{23}=10.37).

For fiber cell quantification experiments, serial transverse frozen sections from wild-type, *Sox1*$^{+/-}$, *Sox1*$^{+/-}$; *Pax6*$^{Sey/+}$ and *Pax6*$^{Sey/+}$ E13.5 embryos were cut through 5 embryos of each genotype. Immunofluorescence for E-cadherin with DAPI nuclear stain was performed to identify epithelial cells. Cells positive for DAPI, but negative for E-cadherin in sections from the central lens were counted and averaged (1-wild-type 222 ± 24 cells; 2-*Sox1*$^{+/-}$ 232 ± 40 cells; 3-*Sox1*$^{+/-}$; *Pax6*$^{Sey/+}$ 190 ± 31 cells, 4-*Pax6*$^{Sey/+}$ 144 ± 13 cells). Pair wise t-tests were performed to determine statistical significance of data ($p_{14} < 0.001$, $p_{34} < 0.001$).

3. Acknowledgements

The authors are grateful to members of the Maas laboratory for helpful discussions and to anonymous reviewers for their helpful comments. The Pax6 antibody developed by A. Kawakami was obtained from the Developmental Studies Hybridoma Bank (NICHD and The University of Iowa). Dr. Robin Lovell-Badge kindly provided the Sox1 antibody. This work was funded by grant R01 EY010123-10 to RLM. ALD was supported by fellowships F32-DE05735, and T32-EY07145 from NEI administered by the Postdoctoral Training Program in the Molecular Bases of Eye Diseases.

References

Aota S, Nakajima N, Sakamoto R, Wantanabe S, Ibaraki N, Okazaki K. Pax6 autoregulation mediated by direct interaction of Pax6 protein with the head surface ectoderm-specific enhancer of the mouse *Pax6* gene. Dev. Biol 2003;257:1–13. [PubMed: 12710953]

Ashery-Padan R, Marquardt T, Zhou X, Gruss P. Pax6 activity in the lens primordium is required for lens formation and correct placement of a single retina in the eye. Genes Dev 2000;14:2701–2711. [PubMed: 11069887]

Berry V, Yang Z, Addison PK, Francis PJ, Ionides A, Karan G, Jiang L, Lin W, Hu J, Yang R, Moore A, Zhang K, Bhattacharya SS. Recurrent 17 bp duplication in PITX3 is primarily associated with posterior polar cataract (CPP4). J. Med. Genet 2004;41:e109. [PubMed: 15286169]

Blixt A, Mahlapuu M, Aitola M, Pelto-Huikko M, Enerback S, Carlsson P. A forkhead gene, FoxE3, is essential for lens epithelial proliferation and closure of the lens vesicle. Genes Dev 2000;14:245–254. [PubMed: 10652278]

Brown A, McKie M, van Heyningen V, Prosser J. The Human PAX6 Mutation Database. Nucleic Acids Res 1998;26:259–264. [PubMed: 9399848]

Brownell I, Dirksen M, Jamrich M. Forkhead Foxe3 maps to the dysgenic lens locus and is critical in lens development and differentiation. Genesis 2000;27:81–93. [PubMed: 10890982]

Chauhan BK, Reed NA, Zhang W, Duncan MK, Kilimann MW, Cvekl A. Identification of genes downstream of Pax6 of the mouse lens using cDNA microarrays. J Biol. Chem 2002;277:11539–11548. [PubMed: 11790784]

Collinson JM, Quinn JC, Buchanan MA, Kaufman MH, Wedden SE, West JD, Hill RE. Primary defects in the lens underlie complex anterior segment abnormalities of the Pax6 heterozygous eye. Proc. Natl. Acad. Sci 2001;98:9688–9693. [PubMed: 11481423]

Collinson JM, Quinn JC, Hill RE, West JD. The roles of Pax6 in the cornea, retina, and olfactory epithelium of the developing mouse embryo. Dev. Biol 2003;255:303–312. [PubMed: 12648492]

Dimanlig PV, Faber SC, Auerbach W, Markarenkova HP, Lang RA. The upstream ectoderm enhancer in Pax6 has an important role in lens induction. Development 2001;128:4415–4424. [PubMed: 11714668]

Donner AL, Episkopou V, Maas RL. *Sox2* and *Pou2f1* interact to control lens and olfactory placode development. Dev. Biol. In press

Duncan MK, Kozmik Z, Cveklova K, Piatigorsky J, Cvelk A. Overexpression of PAX6(5a) in lens fiber cells results in cataract and upregulation of (alpha)5(beta)1 integrin expression. J. Cell Sci 2000;113:3173–3185. [PubMed: 10954416]

Duncan MK, Xie L, David LL, Robinson ML, Taube JR, Cui W, Reneker LW. Ectopic Pax6 expression disturbs lens fiber cell differentiation. Invest. Ophthalmol. Vis. Sci 2004;45:3589–3598. [PubMed: 15452066]

Ekonomou A, Kazanis I, Malas S, Wood H, Alifragis P, Denaxa M, Karagogeos D, Constanti A, Lovell-Badge R, Episkopou V. Neuronal migration and ventral subtype identity in the telencephalon depend on SOX1. PLoS Biol 2005;3:e186. [PubMed: 15882093]

Furuta Y, Hogan BL. BMP4 is essential for lens induction in the mouse embryo. Genes Dev 1998;12:3764–3775. [PubMed: 9851982]

Glaser T, Jepeal L, Edwards JG, Young SR, Favor J, Maas RL. PAX6 gene dosage effect in a family with congenital cataracts, aniridia, anophthalmia and central nervous system defects. Nat. Genet 1994;7:463–471. [PubMed: 7951315]

Graw J. Congenital hereditary cataracts. Int. J. Dev. Biol 2004;48:1031–1044. [PubMed: 15558493]

Grindley JC, Davidson DR, Hill RE. The role of Pax-6 in eye and nasal development. Development 1995;121:1433–1442. [PubMed: 7789273]

Hanson IM, Fletcher JM, Jordan T, Brown A, Taylor D, Adams RJ, Punnett HH, van Heyningen V. Mutations at the PAX6 locus are found in heterogeneous anterior segment malformations including Peters' anomaly. Nat. Genet 1994;6:168–173. [PubMed: 8162071]

Hill RE, Favor J, Hogan BL, Ton CC, Saunders GF, Hanson IM, Prosser J, Jordan T, Hastie ND, van Heyningen V. Mouse small eye results from mutations in a paired-like homeobox-containing gene. Nature 1991;354:522–525. [PubMed: 1684639]

Jamieson RV, Perveen R, Kerr B, Carette M, Yardley J, Heon E, Wirth MG, van Heyningen V, Donnai D, Munier F, Black GC. Domain disruption and mutation of the bZIP transcription factor, MAF, associated with cataract, ocular anterior segment dysgenesis and coloboma. Hum. Mol. Genet 2002;11:33–42. [PubMed: 11772997]

Johansson S, Svineng G, Wennerberg K, Armulik A, Lohikangas L. Fibronectin-integrin interactions. Front. Biosci 1997;2:d126–d146. [PubMed: 9159220]

Kamachi Y, Uchikawa M, Tanouchi A, Sekido R, Kondoh H. Pax6 and SOX2 form a co-DNA-binding partner complex regulates initiation of lens development. Genes Dev 2001;15:1272–1286. [PubMed: 11358870]

Kondoh H, Uchikawa M, Kamachi Y. Interplay of Pax6 and SOX2 in lens development as a paradigm of genetic switch mechanisms for cell differentiation. Int. J. Dev. Biol 2004;48:819–827. [PubMed: 15558474]

Lyon MF, Jamieson RV, Perveen R, Glenister PH, Griffiths R, Boyd y, Glimcher LH, Favor J, Munier FL, Black GC. A dominant mutation with the DNA-binding domain of the bZIP transcription factor Maf causes murine cataract and results in selective alteration of DNA binding. Hum. Mol. Genet 2003;12:585–594. [PubMed: 12620964]

Nagy, A.; Gertsenstein, M.; Vintersten, K.; Behringer, R. Manipulating the mouse embryo: A laboratory manual. Cold Spring Harbor, NY: Cold Spring Harbor Laboratory Press; 2003.

Nishiguchi S, Wood H, Kondoh H, Lovell-Badge R, Episkopou V. Sox1 directly regulates the gamma-crystallin genes and is essential for lens development in mice. Genes Dev 1998;12:776–781. [PubMed: 9512512]

Prosser J, van Heyningen V. PAX6 mutations reviewed. Hum. Mutat 1998;11:93–108. [PubMed: 9482572]

Quinn JC, West JD, Hill RE. Multiple functions for Pax6 in mouse eye and nasal development. Genes Dev 1996;10:435–436. [PubMed: 8600027]

Rajaram N, Kerpolla TK. Synergistic transcription activation by Maf and Sox and their subnuclear localization are disrupted by a mutation in Maf that causes cataract. Mol. Cell Biol 2004;24:5694–5709. [PubMed: 15199128]

Reza HM, Ogino H, Yasuda K. L-Maf, a downstream target of Pax6, is essential for chick lens development. Mech. Dev 2002;116:61–73. [PubMed: 12128206]

Ring BZ, Cordes SP, Overbeek PA, Barsh GS. Regulation of mouse lens fiber cell development and differentiation by the Maf gene. Development 2000;127:307–317. [PubMed: 10603348]

Sakai M, Serria MS, Ikeda H, Yoshida K, Imaki J, Nishi S. Regulation of c-maf gene expression by Pax6 in cultured cells. Nucleic Acids Res 2001;29:1228–1237. [PubMed: 11222774]

Schedl A, Ross A, Lee M, Engelkamp D, Rashbass P, van Heyningen V, Hastie ND. Influence of PAX6 gene dosage on development: overexpression causes severe eye abnormalities. Cell 1996;86:71–82. [PubMed: 8689689]

Semina EV, Ferrell RE, Mintz-Hittner HA, Bitoun P, Alward WL, Reiter RS, Funkauser C, Daack-Hirsch S, Murray JC. A novel homeobox gene PITX3 is mutated in families with autosomal-dominant cataracts and ASMD. Nat. Genet 1998;19:167–170. [PubMed: 9620774]

Semina EV, Murray JC, Reiter R, Hrstka RF, Graw J. Deletion in the promoter region and altered expression of Pitx3 homeobox gene in aphakia mice. Hum. Mol. Genet 2000;9:1575–1585. [PubMed: 10861284]

Semina EV, Brownell I, Mintz-Hittner HA, Murray JC, Jamrich M. Mutations in the human forkhead transcription factor FOXE3 associated with anterior segment ocular dysgenesis and cataracts. Hum. Mol. Genet 2001;10:231–236. [PubMed: 11159941]

van Raamsdonk CD, Tilghman SM. Dosage requirement and allelic expression of PAX6 during lens placode formation. Development 2000;127:5439–5448. [PubMed: 11076764]

Wigle JT, Chowdhury K, Gruss P, Oliver G. Prox1 function is crucial for mouse lens-fibre elongation. Nat Genet 1999;21:318–322. [PubMed: 10080188]

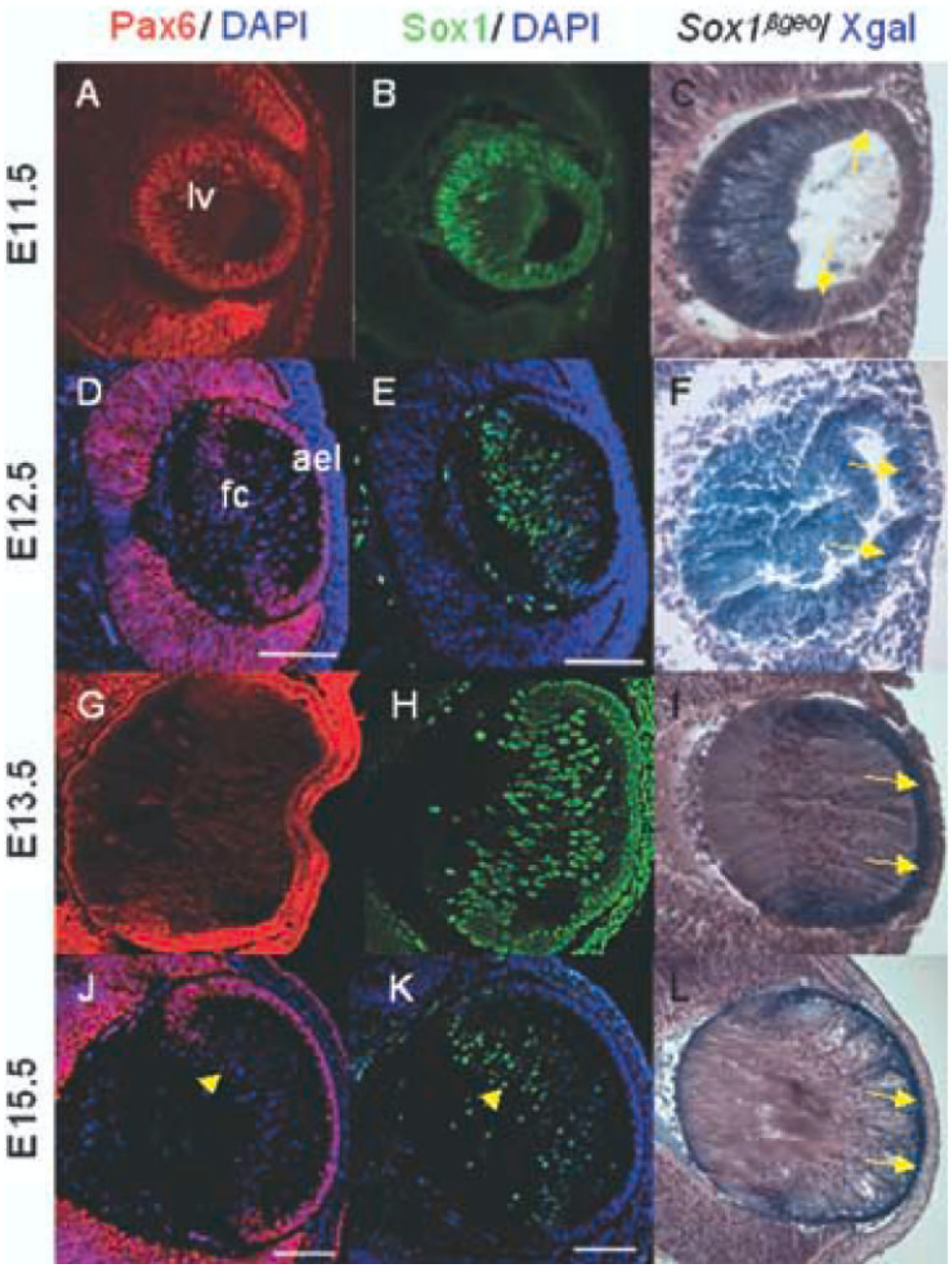

Fig. 1.

Pax6 and Sox1 expression are inversely correlated in the developing fiber cell compartment. Wild-type eyes at embryonic day (E) 11.5 (A–C), E12.5 (D–F), E13.5 (G–I), and E15.5 (J–L) with immunofluorescence for Pax6 (red) (A, D, G, J), or Sox1 (green) (B, E, H, K) and DAPI nuclear stain (blue) are shown. Additional sections of $Sox1^{\beta geo/+}$ lenses stained for β-galactosidase activity are shown (C, F, I, L) to highlight Sox1 expression in the AEL. The arrows in C highlight the anterior extreme of β-galactosidase activity. The arrows in panels F, I and L indicate β-galactosidase activity in the AEL. The arrowheads in J and K highlight nuclei positive for Sox1 and negative for Pax6. All eyes (in all figures) are oriented anterior to the right and posterior to the left. Abbreviations: ael anterior epithelial layer, fc fiber cell compartment, lv lens vesicle Scale bars in all figures are 100 microns.

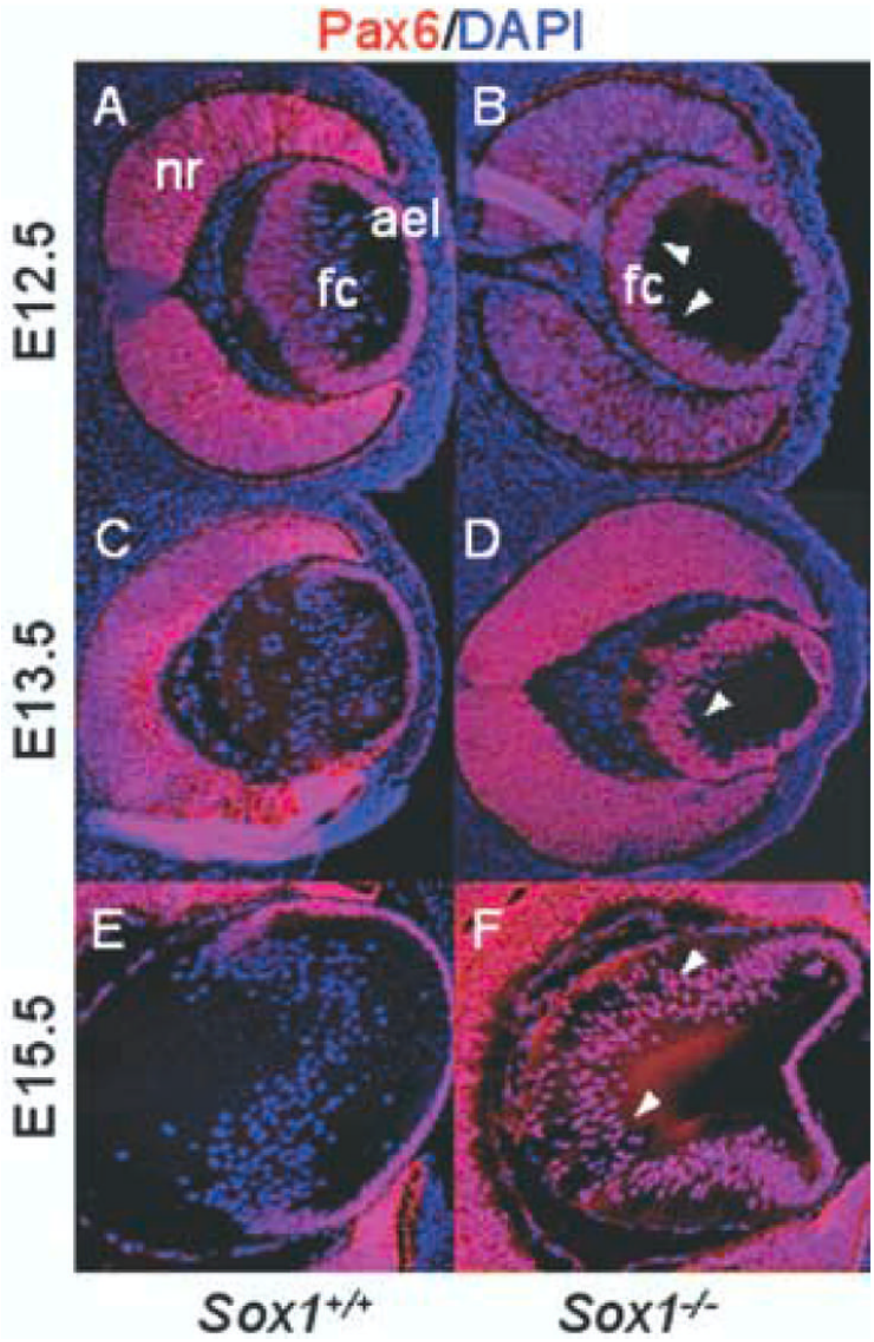

Fig. 2.

Pax6 expression is inappropriately maintained in the fiber cell compartment of *Sox1*$^{-/-}$ lenses. Wild-type (A, C, E) and *Sox1*$^{-/-}$ lenses (B, D, F) are shown with Pax6 immunofluorescence (red) and DAPI nuclear stain (blue) at E12.5 (A–B), E13.5 (C–D), and E15.5 (E–F). Arrowheads indicate fiber cell nuclei positive for Pax6.

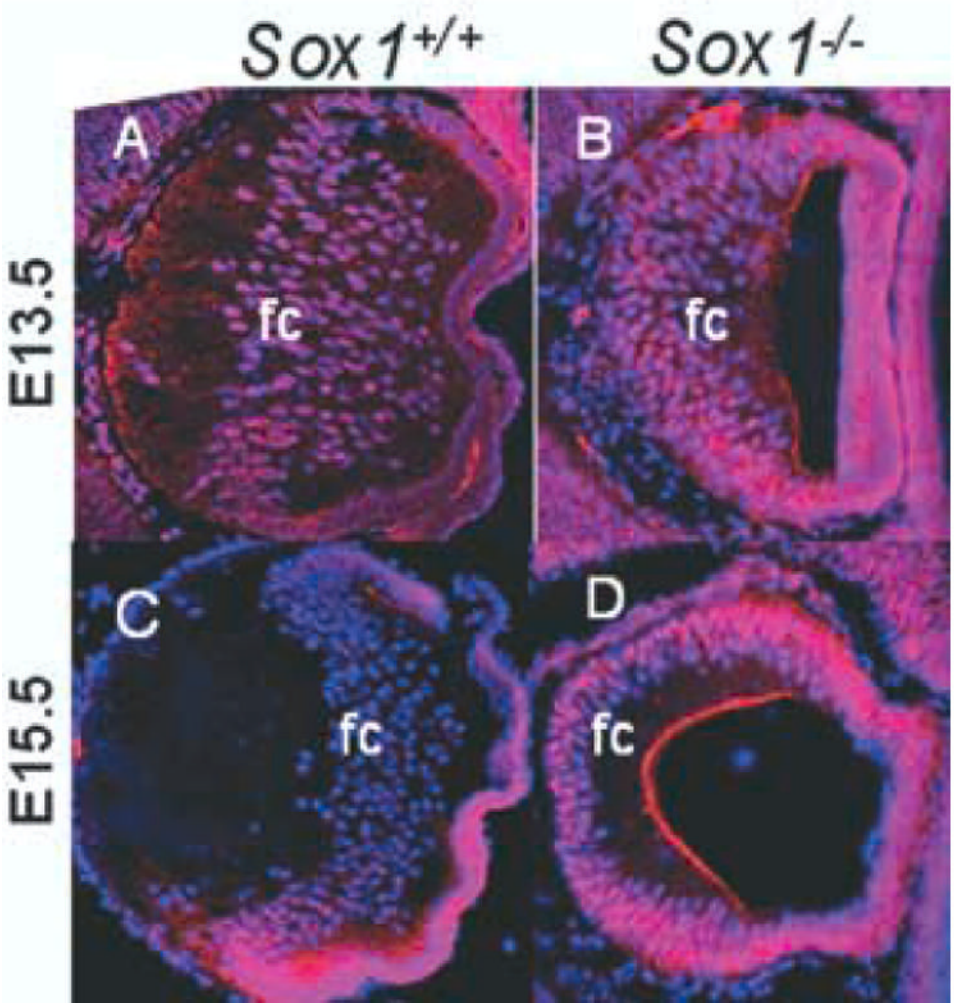

Fig. 3.

α5 integrin, a Pax6 target, is inappropriately maintained in the fiber cell compartment of *Sox1*$^{-/-}$ lenses. Wild-type (A, C) and *Sox1*$^{-/-}$ lenses (B, D) are shown with α5 integrin immunofluorescence (red) and DAPI nuclear stain (blue) at E13.5 (A–B) and E15.5 (C–D). Abbreviations: fc fiber cell compartment

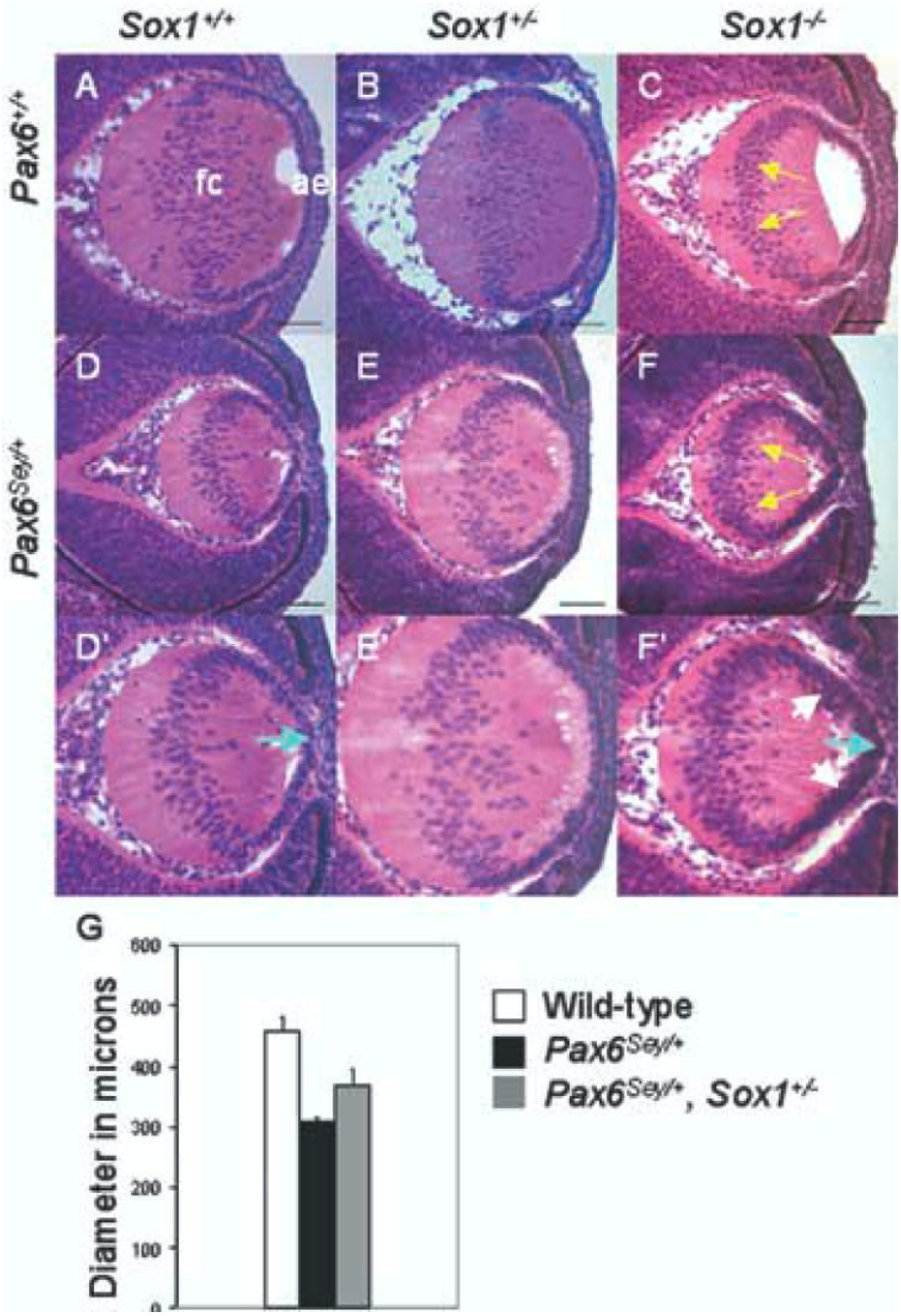

Fig. 4.

Sox1 heterozygosity partially rescues the size of $Pax6^{Sey/+}$ lenses. Representative lenses at E13.5 are shown for wild-type (A); $Sox1^{+/-}$ (B); $Sox1^{-/-}$ (C); $Pax6^{Sey/+}$ (D–D'); $Pax6^{Sey/+}$, $Sox1^{+/-}$ (E–E'); and $Pax6^{Sey/+}$, $Sox1^{-/-}$ (F–F') lenses. High magnification images (D'–F') show epithelial layer abnormalities. Yellow arrows indicate fiber cell nuclei that have remained in the lens posterior (C, F). White arrows indicate multi-layered AEL (F') and blue arrows indicate pointed AEL (D', F'). (G) Maximum lens diameters for wild-type (white box), $Pax6^{Sey/+}$ (black box), and $Pax6^{Sey/+}$, $Sox1^{+/-}$ (gray box) lenses are statistically different (see Experimental Procedures).

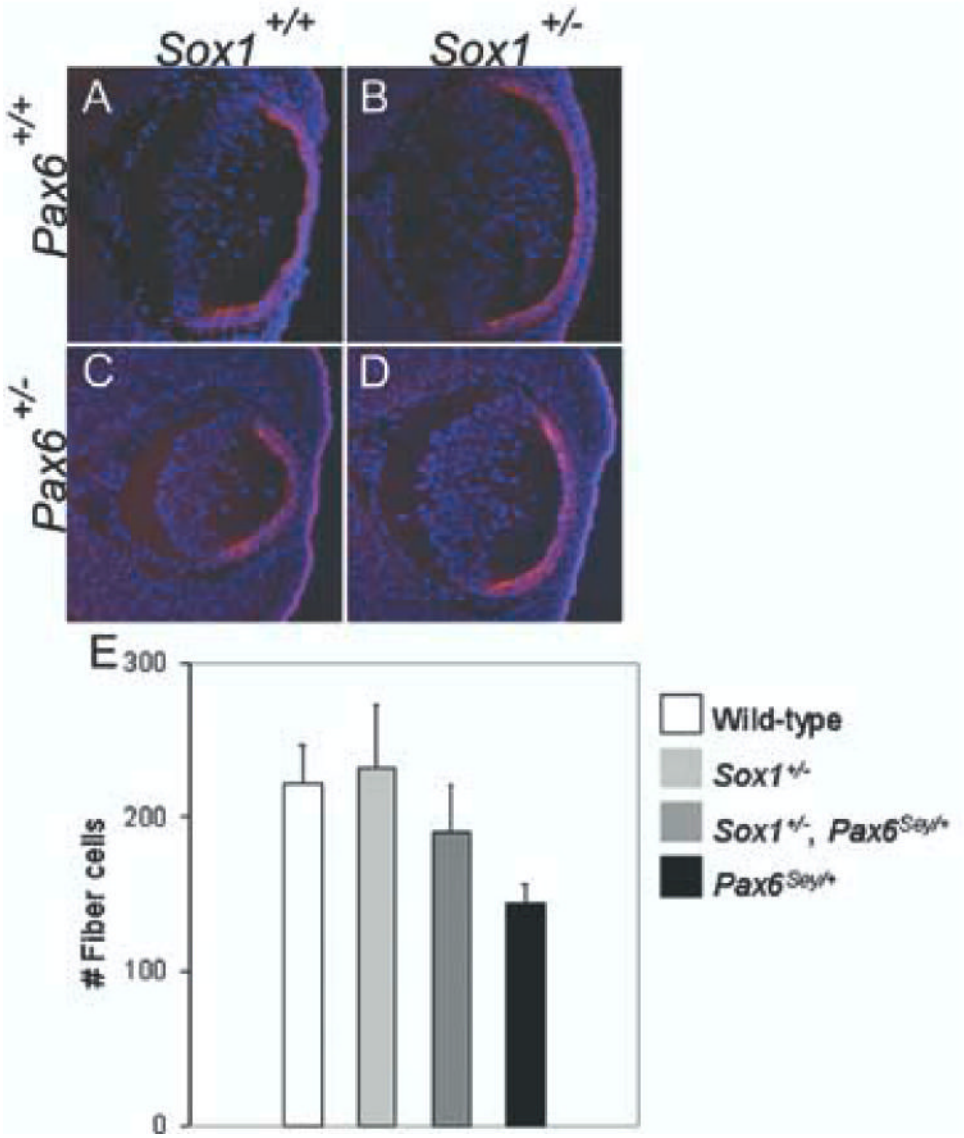

Fig. 5.

Sox1 heterozygosity increases the number of fiber cells in *Pax6*$^{Sey/+}$ lenses. E-cadherin immunofluorescence (red) and DAPI nuclear stain (blue) are shown (A–D) for wild-type (A), *Sox1*$^{+/-}$ (B), *Pax6*$^{Sey/+}$ (C) and *Pax6*$^{Sey/+}$, *Sox1*$^{+/-}$ (D) lenses at E13.5. (E) E-cadherin negative, fiber cell nuclei were counted for wild-type (white box), *Sox1*$^{+/-}$ (light grey box), *Pax6*$^{Sey/+}$ (black box) and *Pax6*$^{Sey/+}$, *Sox1*$^{+/-}$ (dark grey box) lenses and the number of fiber cell nuclei in *Pax6*$^{Sey/+}$, *Sox1*$^{+/-}$ lenses is statistically significantly higher than those in *Pax6*$^{Sey/+}$ lenses (see Experimental Procedures).

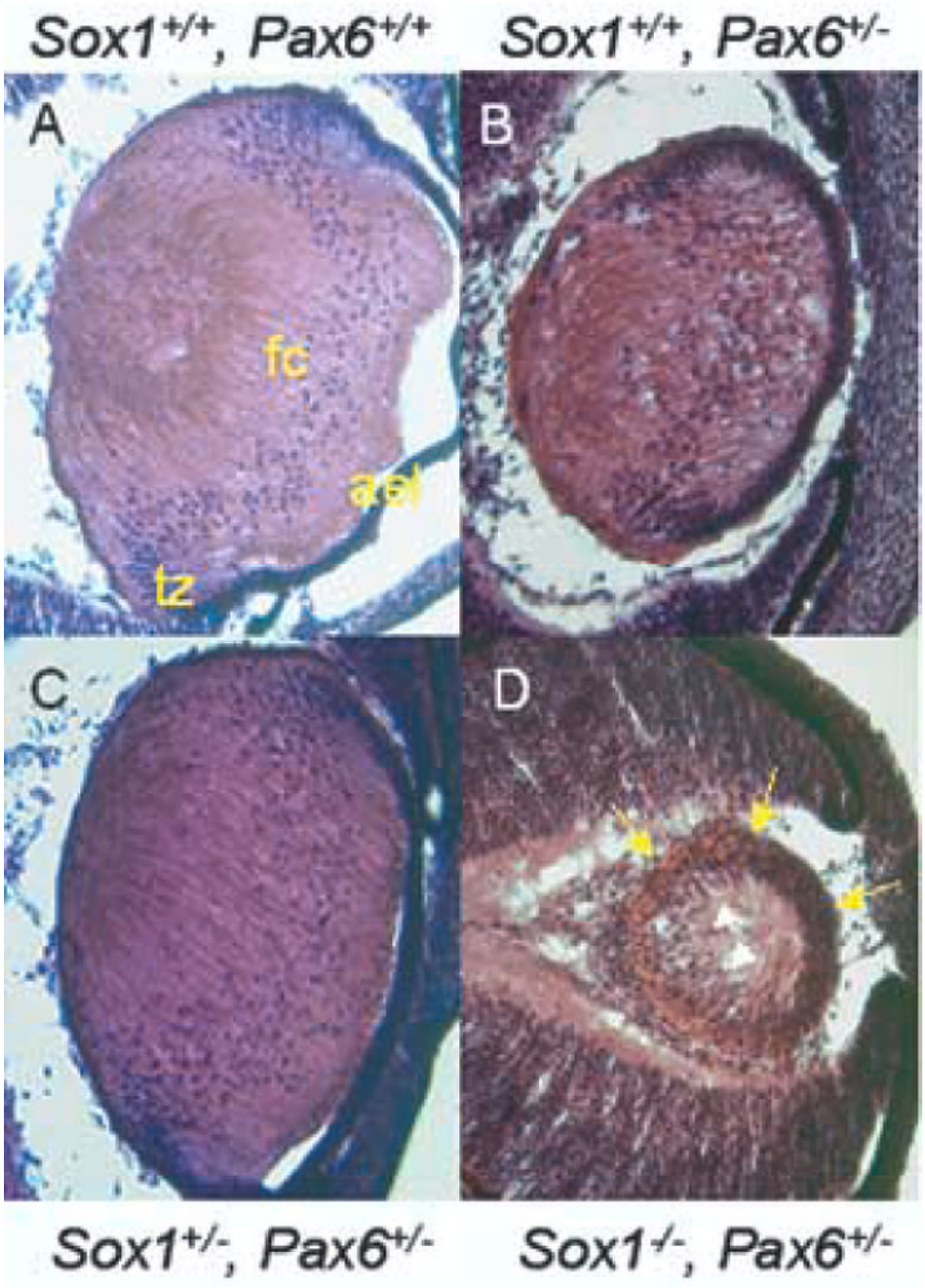

Fig. 6.

Sox1$^{-/-}$*; Pax6*$^{Sey/+}$ lenses have a progressively degenerative phenotype. H&E stained wild-type (A), *Pax6*$^{Sey/+}$ (B), *Sox1*$^{+/-}$*; Pax6*$^{Sey/+}$ (C), and *Sox1*$^{-/-}$*; Pax6*$^{Sey/+}$ (D) E15.5 lenses are shown. Distinct compartments for AEL, transition zone (tz), and fiber cells (fc) are evident in panels A–C. In panel D, yellow arrows indicate uniform appearance of cells around the lens perimeter and white arrows indicate the most anterior nuclei of the lens fiber cell compartment.